Supporting Information for: DFT based microkinetic modeling of confinement driven [4+2] Diels-Alder reactions between ethene and isoprene in H-ZSM5

Christopher Rzepa[1] and Srinivas Rangarajan[1,*]

[1]*Department of Chemical and Biomolecular Engineering, Lehigh University, Bethlehem, PA 18015, USA*

(Dated: September 29, 2022)

* Corresponding Author: srr516@lehigh.edu

SI.I. ENTROPY APPROXIMATIONS AND FREE ENERGY DERIVATION

For molecules that were strongly adsorbed, all modes were assumed to be vibrational with the entropy calculated through it's standard statistical mechanical expression:

$$S^0_{vib} = R\Sigma_i[\frac{h\nu_i}{k_BT(exp(\frac{h\nu_i}{k_BT}-1))} - ln(1-exp(\frac{-h\nu_i}{k_BT}))] \tag{1}$$

Weakly adsorbed systems, particularly those without a direct bond with the acid site, have been shown to exhibit some translational freedom under ambient conditions. As a consequence, the harmonic oscillator approximation would greatly underestimate the entropy of such a loosely bound state. It has been shown that a better approximation includes decoupling the adsorbate's modes into vibrations and two-dimensional free translations about an area commensurate to the pore of MFI (200 pm x 600 pm).[1–4] This includes removing the two smallest frequencies from the vibrational entropy and adding a translational contribution to the entropy given by the following expression:

$$\begin{aligned} S^0_{trans} &= R[ln[(\frac{2\pi M k_B T}{h^2})\frac{A^0}{N_A}] + 2] \\ S^0_{ads} &= S^0_{trans} + S^0_{vib} \end{aligned} \tag{2}$$

Equation 2 assumes that the loosely bound adsorbate is unhindered in translating along a surface and behaves as a 2D ideal gas, where A^0/N_A corresponds to the available surface of an acid site for the adsorbate to freely translate about. These approximations are defined as "Free translator" and "Harmonic Oscillator" within the manuscript respectively. In Table S1, we compare the Harmonic Oscillator and Free Translator against two empirically developed approximations of the adsorption entropy. Namely, that by Campbell and Sellers[5] for hydrocarbons adsorbing on two-dimensional catalytic surfaces; and that by Dauenhauer and Abdelrahman[6] for hydrocarbons within acidic zeolites. Both approximations predicted more positive adsorption entropies relative to our Free Translator approximation. In this study, we chose to strictly work with the Harmonic Oscillator and Free Translor approximations because 1) the Campbell and Sellers approximations is particular for hydrocabron adsorption on two-diemnsional catalytic surfaces and 2) the Dauenhauer and Abdelrahman approximation was developed without any of the reactants and products considered within this study.

	ΔS^0_{ads} [J/mol/K] at 298.15 [J/mol/K]			
adsorbate	**Harmonic Oscillator**	**Free Translator**	**Campbell-Sellers[5]**	**Dauenhauer-Abdelrahman[6]**
physisorbed ethene	-143	-107	-93	-83
physisorbed trans-isoprene	-191	-147	-121	-113
alkoxide ethene	-171	-	-93	-83
alkoxide isoprene	-208	-	-121	-113
carbenium isoprene	-179	-136	-121	-113
physisorbed C7	-203	-157	-130	-117
physisorbed C10-para1	-224	-175	-152	-120
physisorbed C10-para2	-218	-169	-151	-118
physisorbed C10-meta1	-226	-177	-153	-116
physisorbed C10-meta2	-218	-169	-151	-118

Table S1. Comparison among the Harmonic Oscillator and Free translator entropy approximations used within this study with those by Campbell and Sellers[5], and Dauenhauer and Abdelrahman[6]

.

The enthalpies were calculated by taking the sum of the DFT-calculated ground state electronic energy, the zero point vibrational energy, and temperature contributions:

$$\begin{aligned} \Delta H(T) &= \Delta E_{DFT} + \Delta E_{ZPVE} + \Delta H_{10 \longrightarrow T} \\ \Delta E_{ZPVE} &= \frac{1}{2} \Sigma_{i=1}^{modes} h\nu_i \\ \Delta H_{10 \longrightarrow T} &= \int_{10}^{T} C_P dT \end{aligned} \tag{3}$$

The temperature corrections were obtained through numerical integration of the temperature dependent heat capacity from a reference temperature (10K). The heat capacity was quantified through fitting the Shomate equation to a set of entropy values computed along the incremental temperatures. Finally, the standard Gibbs Free Energy was derived from it's classical definition:

$$\Delta G^0(T) = \Delta H^0(T) - T\Delta S^0(T) \tag{4}$$

SI.II. ADSORPTION AND DESORPTION APPROXIMATIONS

We have approximated the thermodynamics of the adsorption/desorption steps by constructing a series of pseudo-transition states which have the entropy of their corresponding adsorbate under the "Free Translator" approximation, and the enthalpy of their ideal-gas

state. Our rationale is that these transition states should feel the effects of confinement (loss in partial translational and complete rotational entropy) but not yet be stabilized by the framework's van der Waals forces. Moreover, such an approximation will ensure that the adsorption/desorption steps are quasi-equilibrated; which is a common assumption. The thermodynamic quantities of these steps are mathematically defined as:

$$\begin{aligned} \Delta S^{0,\ddagger}_{i,ads} &= S^0_{i^*,2D} - (S^0_{i,gas} + S^0_{H+}) \\ \Delta H^{0,\ddagger}_{i,ads} &= (H^0_{i,gas} - H^0_{i,gas}) = 0 \\ \Delta S^{0,\ddagger}_{i,des} &= S^0_{i^*,2D} - (S^0_{i^*}) \\ \Delta H^{0,\ddagger}_{i,des} &= (H^0_{i,gas} - H^0_{i^*}) \end{aligned} \tag{5}$$

SI.III. MICROKINETIC MODEL

An upper and lower bound on each kinetic parameter was derived based on the thermodynamic approximations outlined within section SI.I. The equilibrium constant for each step "i" was defined by the expression:

$$K_i(T) = exp(-\frac{\Delta G^0_i}{RT}) = exp(-\frac{\Delta H^0_i - T\Delta S^0_i}{RT}) \tag{6}$$

Rate coefficients for each elementary step were obtained using transition state theory and were calculated according to the expression:

$$k_i(T) = \frac{k_B T}{h} exp(\frac{\Delta S^{0,\ddagger}_i}{R}) exp(-\frac{\Delta H^{0,\ddagger}_i}{RT}) \tag{7}$$

An isothermal-isobaric, ideal, continuously stirred tank reactor (CSTR) under differential conditions with ideal gas streams was used to model our reaction system:

$$\begin{aligned} \frac{dF_i}{dt} = F_{i,0} - F_i + \Omega_{sites} W(\Sigma_j^{steps^*} \nu_{ij} r_j) + V_{gas}(\Sigma_j^{steps} \nu_{ij} r_j) \\ \Sigma_j^{steps^*} \nu_{ij} r_j = \frac{d\Theta_i}{dt},\ where\ \Theta_i = \frac{N_i^*}{N_{sites}} \\ \Sigma_i \Theta_i + \Theta^* = 1 \\ p_i = p_{tot} \frac{F_i}{\Sigma_{i \in Gas} F_i} \end{aligned} \tag{8}$$

Where F_i represents the molar flow rate of species "i" (mol/s). The generation/consumption terms were segregated between reactions occurring within the gas-phase, given by $\Sigma_j^{steps}\nu_{ij}r_j$, and within the catalyst, given by $\Sigma_j^{steps^*}\nu_{ij}r_j$. The index "j", represents the elementary steps which contain species "i" and each ν_{ij} represents their respective stoichiometric coefficient within that step. The reaction rates within the adsorbed phase were given in terms of fractional surface coverage (mol/mol_{H+}), which was represented by the variable Θ_i and constrained by the site balance. The molar quantity of total acid sites per gram of catalyst was defined by Ω_{sites} ($mol_{H+}/g-cat$) and represented a unit cell containing 47 Si/Al. The weight of catalyst was defined by W ($g-cat$). The volume of the gas phase, V_g, was set equal to the volume occupied by the catalyst mass. The isobaric condition of the reactor was satisfied by including an inert, which ensured that the sum of ideal-gas partial pressures of the reactants and products and inert was 1 (atm). Equation 8 was written for each species, which produced a system of differential equations that have been solved simultaneously using an in-house python code. The volumetric flow rate of our reactor was 1800.0 (mL/hr), with a catalyst mass of 0.1 (g). The MKM was solved used a home-built python code, which we made available on github [https://github.com/chr218/GSA_DA_rxn] and is included with the Supporting Information.

The conversion (ξ), selectivity (S), and yield (Y) are defined by equation 9, where $S(D/R)$ and $Y(D/R)$ represent the selectivity and yield of a product "D" with respect to the consumption of a reactant "R". Mathematically, the selectivity must sum to unity; and the reactant "R" was chosen as isoprene unless specified otherwise.

$$\begin{aligned} \xi_i &= \frac{F_{i,0} - F_i}{F_{i,0}} \\ S(D/R) &= \frac{-\nu_R F_D}{\nu_D \xi_R F_{R,0}} \\ \Sigma_{i=1}^{rxns} S(D_i/R) &= 1 \\ Y(D/R) &= \xi_R S(D/R) \end{aligned} \tag{9}$$

The apparent order "n_i" is defined by equation 10. The MKM was run across five partial pressures, corresponding to multiples of 0.95, 0.98, 1.0, 1.02, 1.05 of the nominal pressure (1 atm). The corresponding $ln(r_i)$ were then fit to the pressures using least squares regression. The apparent order was then calculated by taking the product of the slope of the fit with the nominal pressure of 1 atm.

$$n_i = p_i \frac{\partial ln(r_i)}{\partial p_i} \tag{10}$$

The activation energy "ΔE_{act}" is defined by equation 11, where "R" and "T" represent the universal gas constant and temperature respectively. The reaction temperature was varied at $\pm$ 5 K about the nominal condition, fitting the corresponding $ln(r_i)$ to the temperature using least squares regression. The activation energy was then calculated as the product between the slope of the fit with RT^2, where the temperature was our nominal temperature of 368.15 K. The reaction was the consumption of our limiting reactant, isoprene (C_5H_8).

$$\Delta E_{act} = RT^2 \frac{\partial ln(r_{C_5H_8})}{\partial T} \tag{11}$$

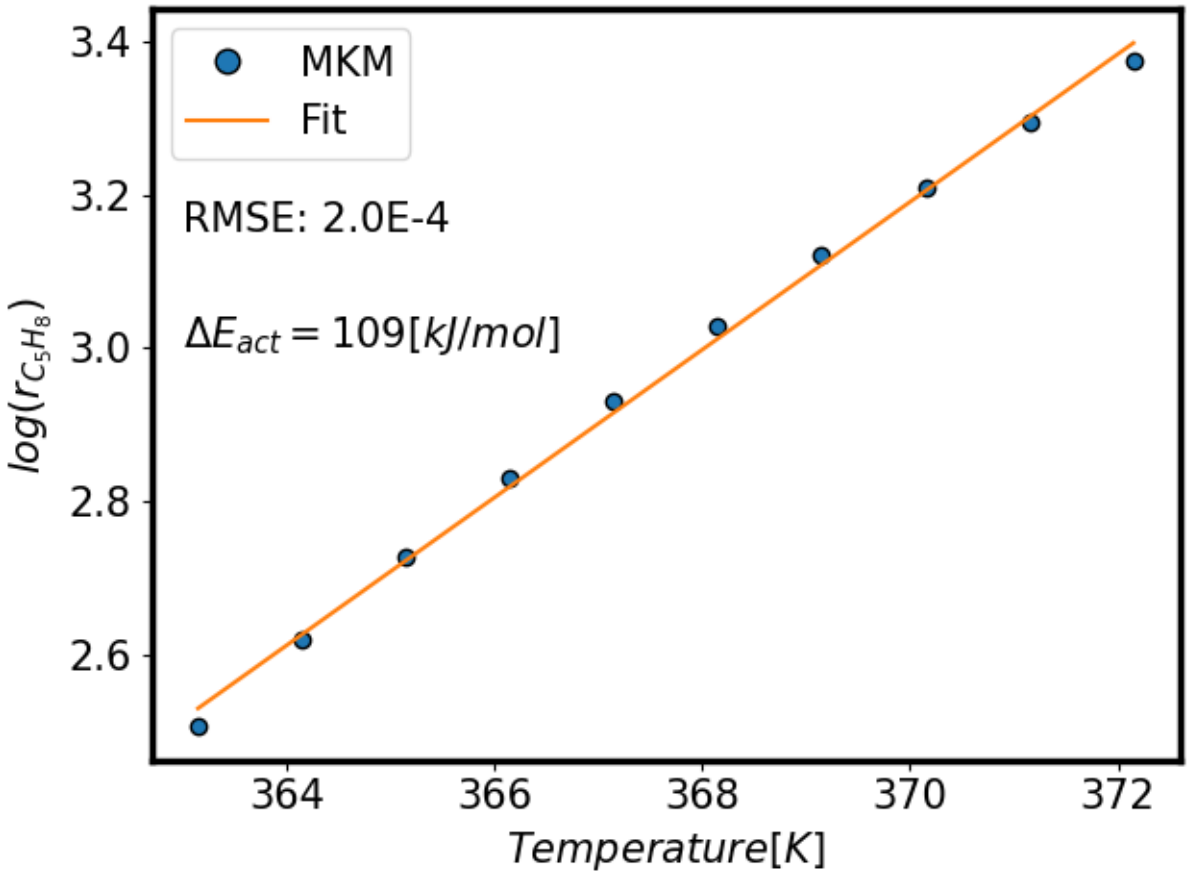

Figure S1. Activation energy of reaction system according to equation 11, with value of 109 kJ/mol. Blue markers represent rate data predicted by MKM. Orange line represents fit of equation 11, with root mean sqaured error of (RMSE) 2.e-04.

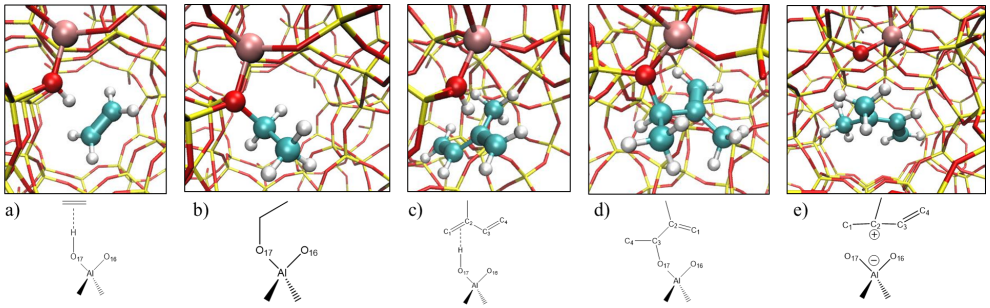

Figure S2. The most energetically stable adsorption configurations of our reactants. The Brønsted proton is bound to O17 for each image; and the aluminum, proton, and oxygen (O17) were emphasized using spheres. The reactant atoms were also represented as spheres, with double bonds emphasized using thicker diameters. Key: silicon (yellow), oxygen (red), hydrogen (white), aluminum (pink), carbon (turquoise) a) Ethene physisorption, where there is a distinct interaction between the Brønsted proton and ethene's double bond. b) Ethene chemisorption, where the primary carbon has been protonated; and an alkoxide bond has formed between O17 and the remaining carbon. c) *Trans*-isoprene physisorption, where the Brønsted proton at the acid site is interacting with the double bond between the primary and tertiary carbons. d) Isoprene chemisorption, where the primary carbon "C_4" has been protonated and an alkoxide bond has formed between the tertiary carbon "C_3"" and O17. e) Carbenium isoprene chemisorption, where the tertiary carbon "C_3" has been protonated.

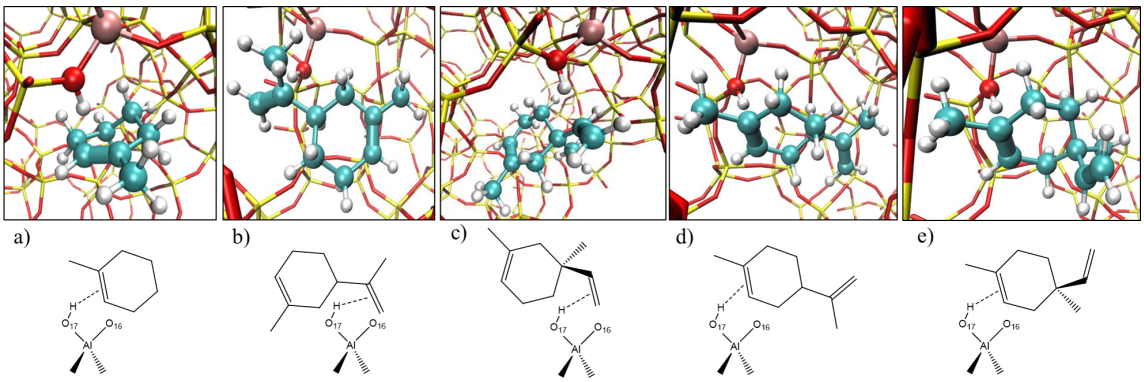

Figure S3. The most energetically stable adsorption configurations of our Diels-Alder products. The Brønsted proton is bound to O17 for each image; and the aluminum, proton, and oxygen (O17) were emphasized using spheres. The reactant atoms were also represented as spheres, with double bonds emphasized using thicker diameters. Key: silicon (yellow), oxygen (red), hydrogen (white), aluminum (pink), carbon (turquoise) a) Product C7 physisorption, where the Brønsted proton interacts with C7's double bond. b) Product C10-meta1 physisorption, where the Brønsted proton interacts with C10-meta1's external double bond. c) Product C10-meta2 physisorption, where the Brønsted proton interacts with C10-meta2's external double bond. d) Product C10-para1 physisorption, where the Brønsted proton interacts with C10-para1's internal double bond. e) Product C10-para2 physisorption, where the Brønsted proton interacts with C10-para2's internal double bond.

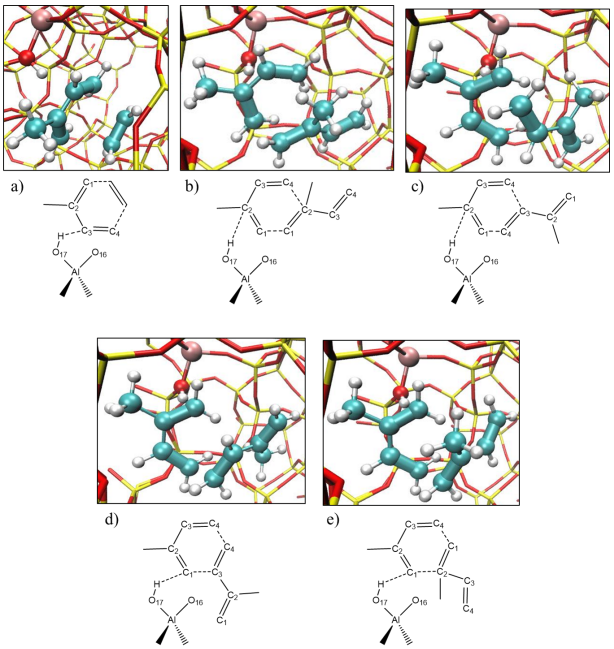

Figure S4. The most energetically stable adsorption configurations of our Diels-Alder transition states (TST). The Brønsted proton is bound to O17 for each image; and the aluminum, proton, and oxygen (O17) were emphasized using spheres. The reactant atoms were also represented as spheres, with double bonds emphasized using thicker diameters. Key: silicon (yellow), oxygen (red), hydrogen (white), aluminum (pink), carbon (turquoise) a) Product C7 TST, where the Brønsted proton interacts with the diene's secondary carbon "C_2". b) Product C10-para2 TST, where the Brønsted proton interacts with the tertiary carbon "C_2" on the diene. c) Product C10-para1 TST, where the Brønsted proton interacts with the tertiary carbon on the diene. d) Product C10-meta1 TST, where the Brønsted proton interacts with the diene's primary carbon "C_1". e) Product C10-meta2 TST, where the Brønsted proton interacts with the diene's primary carbon "C_1".

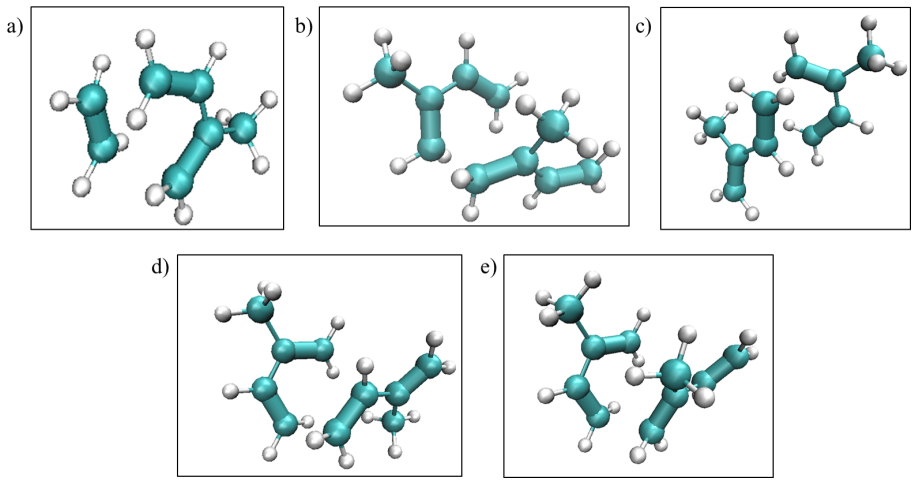

Figure S5. The most energetically stable unadsorbed configurations of our Diels-Alder transition states (TST). a) Product C7 TST, b) Product C10-para2 TST, c) Product C10-para1 TST, d) Product C10-meta1 TST, e) Product C10-meta2 TST.

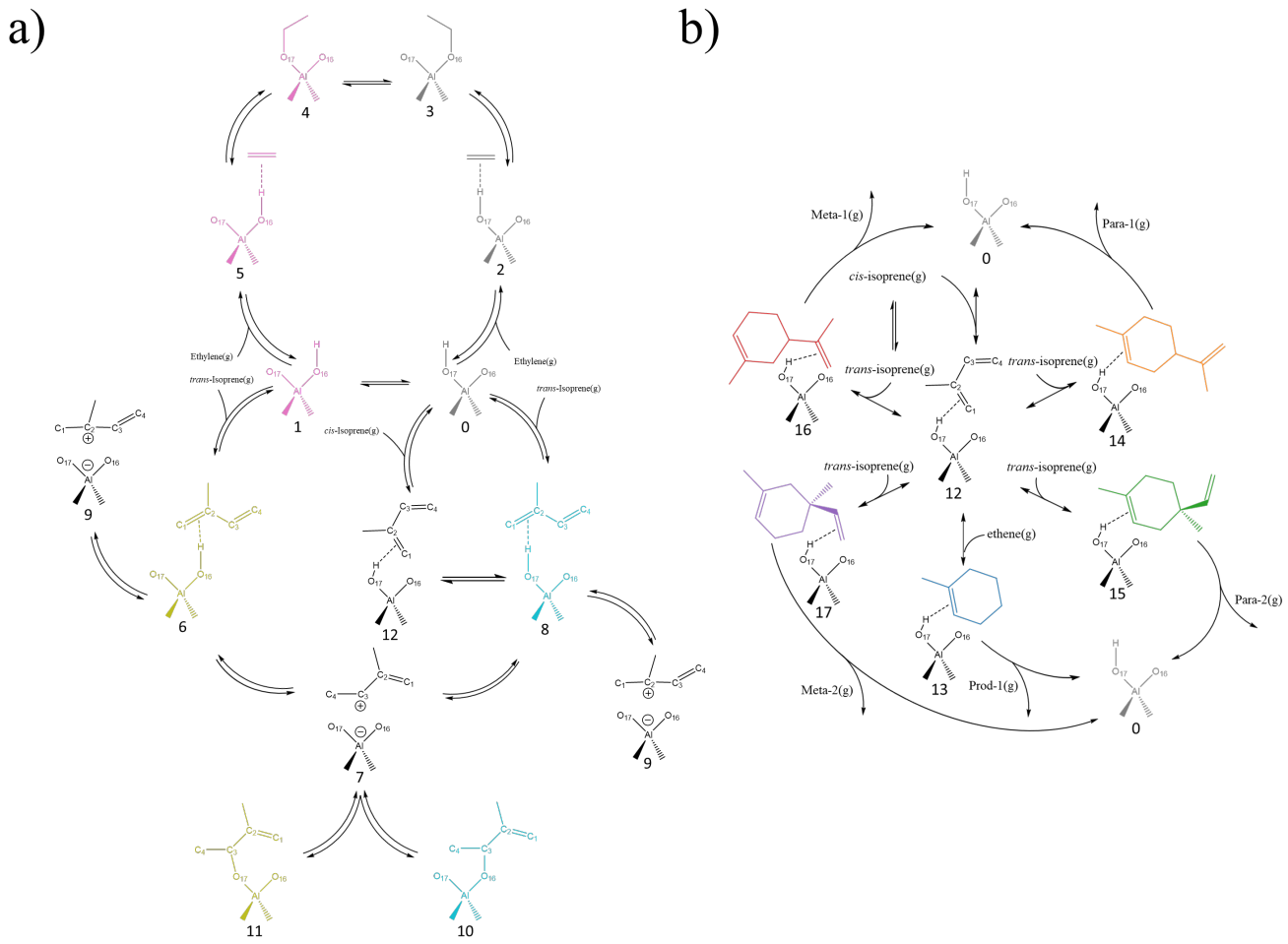

Figure S6. The reaction network, consisting of all catalytic elementary steps within the MKM with the coloring scheme and index for each intermediate having been preserved from the Gibbs free energy surfaces described in the manuscript. Each step is assumed elementary; and is categorized between: a) competitive physisorpion/chemisorption network b) DA cycloaddition network. The corresponding enthalpy, entropy, activation energy, forward rate constant, and equilibrium constants for each step are given in table S2. Gas phase DA reactions were also included within the MKM, but were not listed here.

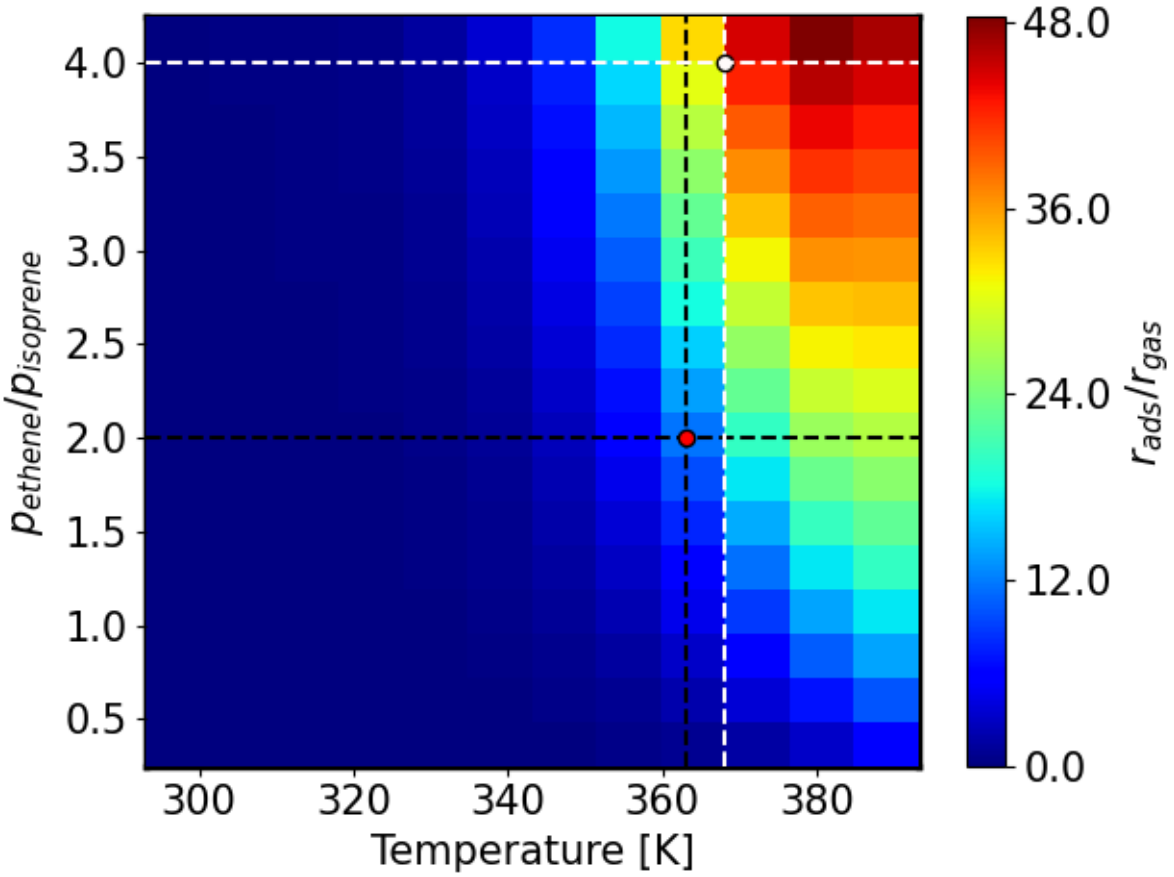

Figure S7. Heatmap of the catalytic flux, against the inlet reactant ratio (dienophile:diene) and temperature (K). The catalytic flux was defined as the ratio of isoprene consumption from the adsorbed phase reactions against the unadsorbed gas-phase reactions. The red and white dots represent the conditions of Bernardon et al.[7] and those used in this paper respectively.

	step	ΔH_r^0	ΔS_r^0	Ea_f	k_f	K_{eq}
r_0	(0)-(1)	10\10\10	1\1\1	58\58\58	5E+04\5E+04\5E+04	4E-02\4E-02\4E-02
r_1	(2)-(3)	-21\-19\-19	-31\-66\-66	101\116\116	4E-02\3E-04\3E-04	2E+01\2E-01\2E-01
r_2	(5)-(4)	-55\-53\-53	-28\-62\-62	64\79\79	6E+03\5E+01\5E+01	2E+06\2E+04\2E+04
r_3	(6)-(7)	15\15\15	1\1\1	21\21\21	9E+09\9E+09\9E+09	7E-03\7E-03\7E-03
r_4	(7)-(11)	-18\-16\-16	-20\-62\-62	12\12\12	1E+11\1E+11\1E+11	3E+01\1E-01\1E-01
r_5	(7)-(10)	0\2\2	-23\-65\-65	26\26\26	1E+09\1E+09\1E+09	7E-02\2E-04\2E-04
r_6	(8)-(7)	35\35\35	2\2\2	39\39\39	2E+07\2E+07\2E+07	2E-05\2E-05\2E-05
r_7	(3)-(4)	-18\-18\-18	2\2\2	129\115\115	3E-06\4E-04\4E-04	4E+02\4E+02\4E+02
r_8	(8)-(12)	14\14\14	3\3\3	30\30\30	4E+08\4E+08\4E+08	2E-02\2E-02\2E-02
r_9	(6)-(9)	11\11\11	11\11\11	34\34\34	1E+08\1E+08\1E+08	1E-01\1E-01\1E-01
r_{10}	(8)-(9)	30\30\30	12\12\12	35\35\35	7E+07\7E+07\7E+07	2E-04\2E-04\2E-04
r_{11}	(12+0g)-(13)	-220\-218\-220	-207\-249\-204	80\79\79	4E+01\5E+01\5E+01	3E+20\9E+17\4E+20
r_{12}	(12+1g)-(14)	-212\-210\-212	-248\-290\-242	91\89\89	8E-01\2E+00\2E+00	1E+17\4E+14\3E+17
r_{13}	(12+1g)-(15)	-215\-213\-215	-246\-288\-240	90\88\88	1E+00\2E+00\2E+00	5E+17\2E+15\1E+18
r_{14}	(12+1g)-(16)	-208\-206\-208	-248\-290\-243	83\81\81	1E+01\2E+01\2E+01	3E+16\1E+14\7E+16
r_{15}	(12+1g)-(17)	-207\-205\-207	-246\-288\-240	81\79\79	2E+01\4E+01\4E+01	3E+16\1E+14\6E+16
r_{16}	(0g+7g)-(2g)	-197\-197\-197	-196\-196\-196	88\88\88	9E+04\9E+04\9E+04	6E+17\6E+17\6E+17
r_{17}	(1g+7g)-(3g)	-172\-172\-172	-216\-216\-216	110\110\110	7E+01\7E+01\7E+01	1E+13\1E+13\1E+13
r_{18}	(1g+7g)-(5g)	-164\-164\-164	-221\-221\-221	115\115\115	1E+01\1E+01\1E+01	6E+11\6E+11\6E+11
r_{19}	(1g+7g)-(4g)	-172\-172\-172	-215\-215\-215	115\115\115	1E+01\1E+01\1E+01	1E+13\1E+13\1E+13
r_{20}	(1g+7g)-(6g)	-167\-167\-167	-221\-221\-221	115\115\115	1E+01\1E+01\1E+01	2E+12\2E+12\2E+12
r_{21}	(1g)-(7g)	16\16\16	5\5\5	31\31\31	1E+13\1E+13\1E+13	9E-03\9E-03\9E-03
r_{22}	(0+0g)-(2)	-57\-59\-59	-141\-106\-106	39\39\39	2E+07\2E+07\2E+07	5E+00\7E+02\7E+02
r_{23}	(1+0g)-(5)	-52\-54\-54	-144\-109\-109	40\40\40	2E+07\2E+07\2E+07	7E-01\8E+01\8E+01
r_{24}	(0+1g)-(8)	-95\-98\-98	-188\-147\-147	54\54\54	2E+05\2E+05\2E+05	5E+03\1E+06\1E+06
r_{25}	(1+1g)-(6)	-86\-89\-89	-188\-147\-147	54\54\54	2E+05\2E+05\2E+05	3E+02\8E+04\8E+04
r_{26}	(0+7g)-(12)	-98\-100\-100	-190\-148\-148	55\55\55	1E+05\1E+05\1E+05	9E+03\3E+06\3E+06
r_{27}	(0+2g)-(13)	-121\-121\-123	-201\-201\-157	58\58\58	5E+04\5E+04\5E+04	4E+06\4E+06\2E+09
r_{28}	(0+3g)-(14)	-138\-138\-140	-222\-222\-175	64\64\64	6E+03\6E+03\6E+03	8E+07\8E+07\5E+10
r_{29}	(0+5g)-(15)	-149\-149\-151	-216\-216\-168	62\62\62	1E+04\1E+04\1E+04	7E+09\7E+09\4E+12
r_{30}	(0+4g)-(16)	-134\-134\-136	-224\-224\-177	65\65\65	5E+03\5E+03\5E+03	2E+07\2E+07\1E+10
r_{31}	(0+6g)-(17)	-137\-137\-139	-216\-216\-168	62\62\62	1E+04\1E+04\1E+04	2E+08\2E+08\1E+11

Table S2. Standard reaction enthalpy (kJ/mol), reaction entropy ($J/mol/K$), activation energy (kJ/mol), foreword rate constant (s^{-1}) and equilibrium constant ($dimensionless$) for each elementary reaction step outlined within Figure S6 at 368.15 (K). The lower and upper bounds are given by the HO and Free Translator approximations defined in section SI.I, including an additional approximation where the adsorbate entropies are estimated using the Free Translator with the exception of the adsorbed cycloadducts, which are approximated by the HO. These three approximations are ordered: HO/(Free Translator & HO)/Free Translator within the table. Gas phase DA reactions were also included within the MKM; and are represented by r_{16-21}, which correspond to C7, C10-para1, C10-para2, C10-meta1, C10-meta2 product formation and *trans*-isoprene isomerization to *cis*-isoprene.

adsorbate	Conversion %	Yield %	Selectivity %	Fractional Coverage
ethene	0.2/0.2/0.01	-	-	6.8E-2/3.4E-4/5.7E-7
isoprene	1.1/1.3/0.04	-	-	1.6E-3/1.1E-3/1.8E-6
C7	-	0.8/0.8/0.03	69.9/62.3/97.7	2.0E-2/8.9E-3/6.2E-3
C10-para1	-	0.01/0.01/<0.001	0.7/0.9/0.09	9.5E-3/1.2E-2/1.2E-2
C10-para2	-	0.1/0.2/<0.001	10.3/12.9/0.79	6.0E-1/6.5E-1/6.6E-1
C10-meta1	-	0.01/0.02/<0.001	1.0/1.3/0.08	4.1E-2/5.0E-2/5.1E-2
C10-meta2	-	0.2/0.3/<0.001	18/23/1.4	2.6E-1/2.7E-1/2.8E-1

Table S3. The conversion, selectivity, and coverage per adsorbate quantified from the MKM under the entropic approximations discussed within SI.I, including an additional approximation where the adsorbate entropies are estimated using the Free Translator with the exception of the adsorbed cycloadducts, which are approximated by the HO. These three approximations are ordered: HO/(Free Translator & HO)/Free Translator within the table. The isoprene conversion included both isomers (*cis*− and *trans*−). The coverage for ethene and isoprene included their physisorbed, chemisorbed, and carbenium states on O17 and O16, including both isomers of isoprene (*cis*− and *trans*−). The conversion, yield, and selectivity between 1) the Free Translator & HO and 2) the HO, were much more similar relative to the Free Translator approximation. The coverage under the Free Translator & HO was more similar to the Free Translator approximation for the cycloadducts, but more similar to the HO for the reactants.

	step	$r_{foreward}$	$r_{reverse}$	r_{net}
r_0	(0)-(1)	6E+04\3E+02\5E-01	6E+04\3E+02\5E-01	7E-01\7E-01\1E-03
r_1	(2)-(3)	3E-02\2E-04\3E-07	3E-02\2E-04\3E-07	7E-10\7E-08\1E-10
r_2	(5)-(4)	3E+01\1E-01\2E-04	3E+01\1E-01\2E-04	-7E-10\-7E-08\-1E-10
r_3	(6)-(7)	4E+09\3E+09\4E+06	4E+09\3E+09\4E+06	7E-01\7E-01\1E-03
r_4	(7)-(11)	5E+08\3E+08\5E+05	5E+08\3E+08\5E+05	2E-07\-6E-08\-1E-08
r_5	(7)-(10)	5E+06\3E+06\6E+03	5E+06\3E+06\6E+03	0E+00\1E-09\-7E-11
r_6	(8)-(7)	4E+09\3E+09\4E+06	4E+09\3E+09\4E+06	-7E-01\-7E-01\-1E-03
r_7	(3)-(4)	7E-05\4E-05\7E-08	7E-05\4E-05\7E-08	7E-10\7E-08\1E-10
r_8	(8)-(12)	8E+10\6E+10\1E+08	8E+10\6E+10\1E+08	2E+01\2E+01\3E-02
r_9	(6)-(9)	6E+07\4E+07\7E+04	6E+07\4E+07\7E+04	2E-02\2E-02\3E-05
r_{10}	(8)-(9)	1E+10\1E+10\2E+07	1E+10\1E+10\2E+07	-2E-02\-2E-02\-4E-05
r_{11}	(12+0g)-(13)	1E+01\1E+01\2E-02	3E-16\7E-14\1E-16	1E+01\1E+01\2E-02
r_{12}	(12+1g)-(14)	7E-02\1E-01\2E-04	8E-15\5E-12\9E-15	7E-02\1E-01\2E-04
r_{13}	(12+1g)-(15)	1E-01\1E-01\2E-04	2E-13\1E-10\2E-13	1E-01\1E-01\2E-04
r_{14}	(12+1g)-(16)	1E+00\1E+00\2E-03	2E-12\1E-09\2E-12	1E+00\1E+00\2E-03
r_{15}	(12+1g)-(17)	2E+00\3E+00\4E-03	2E-11\1E-08\2E-11	2E+00\3E+00\4E-03
r_{16}	(0g+7g)-(2g)	6E-01\6E-01\6E-01	8E-18\8E-18\3E-19	6E-01\6E-01\6E-01
r_{17}	(1g+7g)-(3g)	1E-04\1E-04\1E-04	1E-18\2E-18\5E-21	1E-04\1E-04\1E-04
r_{18}	(1g+7g)-(5g)	2E-05\2E-05\2E-05	7E-18\1E-17\2E-20	2E-05\2E-05\2E-05
r_{19}	(1g+7g)-(4g)	2E-05\2E-05\2E-05	3E-18\4E-18\7E-21	2E-05\2E-05\2E-05
r_{20}	(1g+7g)-(6g)	2E-05\2E-05\2E-05	4E-17\6E-17\1E-19	2E-05\2E-05\2E-05
r_{21}	(1g)-(7g)	6E+10\6E+10\7E+10	6E+10\6E+10\7E+10	5E-01\5E-01\6E-01
r_{22}	(0+0g)-(2)	3E+06\2E+04\3E+01	3E+06\2E+04\3E+01	2E-09\7E-08\1E-10
r_{23}	(1+0g)-(5)	1E+05\5E+02\8E-01	1E+05\5E+02\8E-01	-8E-10\-7E-08\-1E-10
r_{24}	(0+1g)-(8)	6E+03\3E+01\5E-02	6E+03\2E+01\3E-02	2E+01\2E+01\3E-02
r_{25}	(1+1g)-(6)	3E+02\1E+00\2E-03	3E+02\6E-01\1E-03	7E-01\7E-01\1E-03
r_{26}	(0+7g)-(12)	5E+01\2E-01\4E-04	5E+01\1E-01\2E-04	1E-01\1E-01\2E-04
r_{27}	(0+2g)-(13)	2E+01\8E-02\6E-06	3E+01\1E+01\2E-02	-1E+01\-1E+01\-2E-02
r_{28}	(0+3g)-(14)	1E-02\6E-05\3E-10	8E-02\1E-01\2E-04	-7E-02\-1E-01\-2E-04
r_{29}	(0+5g)-(15)	3E-02\2E-04\6E-10	1E-01\1E-01\2E-04	-1E-01\-1E-01\-2E-04
r_{30}	(0+4g)-(16)	1E-01\7E-04\2E-09	1E+00\1E+00\2E-03	-1E+00\-1E+00\-2E-03
r_{31}	(0+6g)-(17)	5E-01\4E-03\1E-08	2E+00\3E+00\4E-03	-2E+00\-3E+00\-4E-03

Table S4. The foreward, reverse, and net rate (μ-mol/hr) from the MKM with respect to the numbering scheme in S6 under the entropic approximations discussed within SI.I, including an additional approximation where the adsorbate entropies are estimated using the Free Translator with the exception of the adsorbed cycloadducts, which are approximated by the HO. These three approximations are ordered: HO/(Free Translator & HO)/Free Translator within the table. The net rates within the Free Translator & HO approximation more closely resemble the net rates under the HO approximation. Gas phase DA reactions were also included within the MKM; and are represented by r_{16-21}, which correspond to C7, C10-para1, C10-para2, C10-meta1, C10-meta2 product formation and *trans*-isoprene isomerization to *cis*-isoprene.

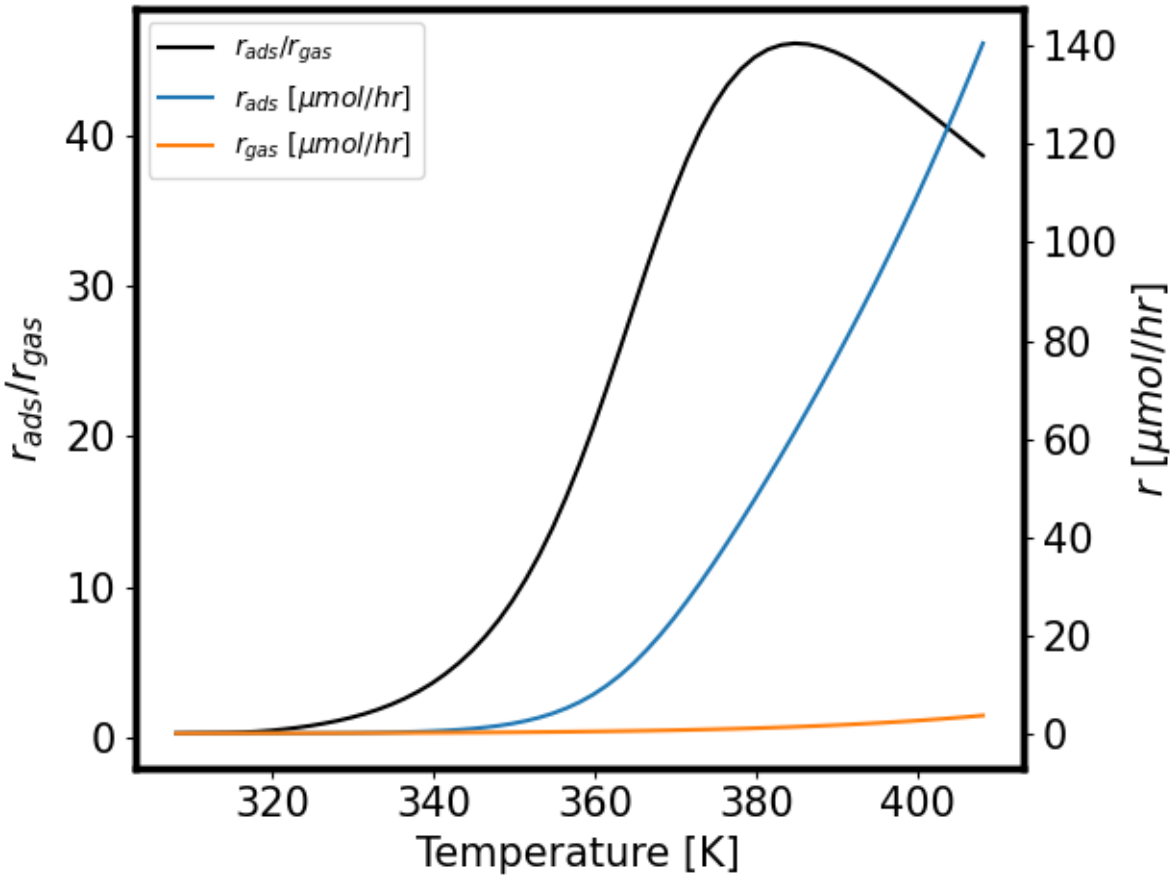

Figure S8. Plot of the reaction flux ratio (r_{ads}/r_{gas}) and rates r_{ads}, r_{gas}, under the HO approximation, of the consumption of isoprene in the adsorbed and unadsorbed gas phases respectively. ($\mu - mol/hr$)

[1] De Moor, B. A.; Reyniers, M.-F.; Sierka, M.; Sauer, J.; Marin, G. B. Physisorption and Chemisorption of Hydrocarbons in H-FAU Using QM-Pot(MP2//B3LYP) Calculations. *The Journal of Physical Chemistry C* **2008**, *112*, 11796–11812.

[2] De Moor, B. A.; Reyniers, M.-F.; Marin, G. B. Physisorption and chemisorption of alkanes and alkenes in H-FAU: a combined ab initio–statistical thermodynamics study. *Phys. Chem. Chem. Phys.* **2009**, *11*, 2939–2958.

[3] De Moor, B. A.; Ghysels, A.; Reyniers, M.-F.; Van Speybroeck, V.; Waroquier, M.; Marin, G. B. Normal Mode Analysis in Zeolites: Toward an Efficient Calculation of Adsorption Entropies. *Journal of Chemical Theory and Computation* **2011**, *7*, 1090–1101, PMID: 26606357.

[4] De Moor, B. A.; Reyniers, M.-F.; Gobin, O. C.; Lercher, J. A.; Marin, G. B. Adsorption of C2-C8 n-Alkanes in Zeolites. *The Journal of Physical Chemistry C* **2011**, *115*, 1204–1219.

[5] Campbell, C. T.; Sellers, J. R. V. The Entropies of Adsorbed Molecules. *Journal of the American Chemical Society* **2012**, *134*, 18109–18115, PMID: 23033909.

[6] Dauenhauer, P. J.; Abdelrahman, O. A. A Universal Descriptor for the Entropy of Adsorbed Molecules in Confined Spaces. *ACS Central Science* **2018**, *4*, 1235–1243, PMID: 30276258.

[7] Bernardon, C.; Louis, B.; Bénéteau, V.; Pale, P. Diels–Alder Reaction between Isoprene and Methyl Acrylate over Different Zeolites: Influence of Pore Topology and Acidity. *ChemPlusChem* **2013**, *78*, 1134–1141.